

Characterization of Polymer Particles via Dynamic Light Scattering and Diffusion Ordered Spectroscopy Techniques

A Mini-Thesis

Submitted to the LSU IGERT Program in fulfillment of the Apprenticeship Project

By

Nadia J. Edwin

December 10, 2001

Dedication

Being the first to do anything can be scary, but with it comes great joy.

I dedicate this mini-thesis to William B. Lee; your work as the first IGERT coordinator will always be remembered.

Acknowledgments

Summers are typically regarded as ‘off-time’ from all things strenuous and engaging. My first summer at Louisiana State University will always be referenced as a time filled with energy and excitement and when working in the lab brought overwhelming satisfaction. I owe this rewarding experience to my professor, Dr. Paul Russo, for taking the time to guide me through that initial research stage and for this I thank him.

I am greatly indebted to my family for their continual support and well wishes. My appreciation and thanks also extends to my lab family: Sibel Turksen, Garrett Doucet and Rafael Cueto, for advice, support and warm friendship.

What would summer weekends be without friends to go bicycle riding and the movies with? To all my friends and associates, my heartfelt thanks.

Finally, I wish to thank the LSU Chemistry Department and the National Science Foundation – IGERT Program for financial support.

Table of Contents

| | |
|---|-----|
| Dedication | ii |
| Acknowledgment | iii |
| Chapter I General Introduction | 5 |
| Chapter II | 8 |
| Light Scattering Characterization of Polymer Particle (CONFIDENTIAL STUDY) | |
| Introduction, 9 | |
| Results and Discussion, 10 | |
| Summary, 17 | |
| Acknowledgment, 17 | |
| Appendix, 18 | |
| Recommendations for Future Studies, 19 | |
| Chapter III | 20 |
| Diffusion Ordered Spectroscopy of Hydroxypropyl Cellulose | |
| Introduction, 21 | |
| Results and Discussion, 22 | |
| Appendix, 23 | |
| Recommendations for Future Studies, 23 | |
| Acknowledgments, 24 | |
| References, 24 | |

CHAPTER I

General Introduction

General Introduction

The final goal of this apprenticeship project is to be exposed to powerful diffusion tools like Dynamic Light Scattering (DLS), Diffusion Ordered Spectroscopy (DOSY) and Fluorescence Photobleaching Recovery (FPR) used to determine the physical properties of macromolecules. It is necessary to master these techniques in order to perform experiments independently. In order to learn how to use these instruments, first, some simple experiments were done to observe the practical applications while simultaneously learning the background and elementary theories. Although these experiments were designed to be simple, emphasis was placed on precision and using proper lab techniques. Skills such as error recognition, repetition of experiments to eliminate 'doubtful' results, ability to correlate results from different experiments were all learned. Two experimental results are provided to demonstrate that an understanding of the instruments was accomplished.

Natural diffusion is a transport process in which there is a net flow of molecules from a region of high concentration to one of low concentration. A. Fick proposed that the flow of matter along a concentration gradient should be analogous to the law of heat flow along a temperature gradient.¹ The product of diffusion coefficient and concentration gradient is a measure of the flux and can be seen in the equation below, known as Fick's first law of diffusion:

$$J = - D_m \left(\frac{dC}{dx} \right)$$

where J represents the flux with units of square centimeter per second, C has concentration units, and D_m is the (translational) diffusion coefficient with units of centimeter squared per second. The subscript represents mutual diffusion coefficient and it is the diffusion coefficient obtained from measuring relaxation of the concentration gradient. Dynamic light scattering is a useful technique for the measurement of motion of molecules by the fluctuations in intensity autocorrelation function of the scattered light. The autocorrelation function, $g^{(1)}(\tau)$ contains information from its distribution of the relaxation rate that can be used to determine molecular size. The decay is that of a single exponential:

$$g^{(1)}(\tau) = \exp(-\Gamma\tau)$$

where Γ is the decay rate. The decay rate is related to the apparent mutual diffusion coefficient by:

$$D_{app} = \Gamma/q^2$$

where q is the scattering vector, $q = (4\pi n/\lambda) \sin(\theta/2)$, n is the refractive index of the solution and the scattering angle is 2θ . The apparent mutual diffusion coefficient can then be used to evaluate the apparent hydrodynamic radius, $R_{h,app}$ of molecules via the Stokes-Einstein equation:

$$R_{h,app} = \frac{kT}{(6\pi\eta D_{app})}$$

where k is the Boltzmann's constant, and η is the solvent viscosity at temperature T .

In addition to the mutual diffusion, there exists a self-diffusion that also depends on concentration, but self diffusion happens even without a concentration gradient. The appropriate relationship is due to Einstein and is appears in the equations below:

$$\langle x^2 \rangle = 2Dt$$

$$D_s = \frac{\langle x^2 \rangle}{2t}$$

The self-diffusion coefficient is referred to as optical tracer self-diffusion coefficient when optical methods such as fluorescence photobleaching recovery experiments are used to obtain it. The FPR apparatus is set up such that either a spot or fringed pattern is bleached on the sample. The fringe pattern is obtained by using a Ronchi ruling at the back focal plane of the microscope objective lens. After bleaching, a striped image resulting from the fringed pattern is written in the sample. In this experiment, an ac voltage, representing the contrast of the pattern, decays exponentially at a rate proportional to the diffusion coefficient: $\text{ac volts} = \exp(-\Gamma t)$ with $\Gamma = DK^2$ where D is the tracer self diffusion coefficient, K is the grating constant, $K = 2\pi/L$ (L is the period of the repeat pattern) and t is the time since photobleach.³ A distinguishing factor observed between mutual and self-diffusion is that for mutual diffusion, the polymer concentration creates fluctuations that help drive the diffusion from a region of high concentration to one of low concentration, while for self-diffusion, the concentration fluctuation remains almost uniform. This behavior is observed because in FPR, the concentration of polymer is proportional to the concentration of dye before bleaching. After bleaching, the concentration of the polymer does not change, while that of the dye changes due to diffusion. The diffusion coefficient is obtained as the slope of Γ versus K^2 plots of the data. Like DLS, the Stokes-Einstein relation, $D_s = k_B T / (6\pi \eta R_h)$ is used to obtain size information.

Diffusion-ordered spectroscopy (DOSY) also provides the self-diffusion coefficient of molecules by separating NMR signals of different species. In this experiment, spin echo spectra measured with different pulsed (magnetic) field gradient strengths and signal decays are analyzed to provide the diffusion coefficients of various species, separated by their NMR chemical shift. The Stokes-Einstein relation is then used to determine molecular size and shape.

References:

- (1) Tanford, Charles. *Physical Chemistry of Macromolecules*; John Wiley & Sons, Inc., New York, 1961.
- (2) Yamakawa, H. *Modern Theory of Polymer Solutions*; New York; Harper & Row, Publishers, Inc., New York, 1971.
- (3) Bu, Z.; Russo, P. S. *Macromolecules* **1994**, *27*, 1187.

(4) Cantor, C.R., Shimmel, P.R. *Biophysical Chemistry*; W.H. Freeman & Co., NY, 1980.

(5) Kazanis, S. *Measuring Diffusion By NMR*, Bruker Instruments Inc., 2000.

CHAPTER II

Light Scattering Characterization of Polymer Particles

(CONFIDENTIAL)

Light Scattering Characterization of Polymer Particles

Introduction

We received two suspensions of particles in THF, each containing about 15 ml at a claimed concentration of 1.2 mg/ml. The XXX product labeled “XXX” is referred to as the “larger” particle. The XXX product labeled “XXX” is referred to as the “smaller” particle. The particles were analyzed blind—i.e., with minimal information as to their chemistry or makeup—by dynamic light scattering (DLS) and by gel permeation chromatography with multiple angle light scattering detection (GPC/MALLS).

Background

For a true sphere, the hydrodynamic radius, R_h , equals the actual radius, R . The radius of gyration, R_g , is given by $(3/5)^{1/2}R$. The hydrodynamic radius is determined from the diffusion coefficient, D , according to the Stokes-Einstein law.

$$R_h = \frac{kT}{(6\pi\eta D_{app})} \quad (1)$$

in which k = Boltzmann's constant, T = the Kelvin temperature, and η = the solvent viscosity.

Measurement of D is done most easily by DLS, which measures the intensity autocorrelation function, $g^{(2)}(t)$ of light scattered by the molecules in solution. One must extrapolate to zero concentration, c , and zero scattering vector magnitude, q . For the conditions of our measurement, the intensity autocorrelation function is converted to the electric field autocorrelation function, $g^{(1)}(t)$ through the Siegert relation. For a single scattering species, the result is a single exponential decay, with decay rate Γ :

$$g^{(1)}(t) = e^{-\Gamma t} \quad (2)$$

The decay rate is directly proportional to the diffusion coefficient, with the constant of proportionality equal to the squared scattering vector magnitude, q^2 :

$$\Gamma = q^2 D \quad (3)$$

One therefore expects a plot of Γ vs. q^2 to be linear with a zero intercept and slope D . As this is often the case, the quantity $D_{app} = \Gamma / q^2$ is computed. A plot of D_{app} vs. q^2 should be flat. Failure of Γ vs. q^2 to rise linearly, or a slanted D_{app} vs. q^2 plot, indicates particle heterogeneity and/or a shape other than spherical.

GPC/MALLS provides absolute molecular weight and particle radius of gyration for each of many slices eluting from a GPC column. When a distribution of polymers exists, this

information can be used to infer particle shape via the scaling relationship between mass and size.

$$M \propto R_g^{d_f} \quad (4)$$

where d_f is the mass fractal dimension. This is often obtained from the slope of a log-log plot of M vs. R_g (or from the inverse of the plot of R_g vs. M). For solid particles, we expect $d_f = 3$, for rods $d_f = 1$, and for random flight polymers in theta conditions $d_f = 2$. For random flight polymers in good solvent conditions, $d_f = 5/3 \cong 1.7$. Branched polymers usually exhibit d_f between $5/3$ and 3 . It is common to discuss the inverse of d_f , which is known as the Flory exponent, ν .

$$\nu = 1/d_f \quad (5)$$

Results & Discussion

DLS. Both large and small particles were exceptionally uniform according to DLS, yielding single exponential decays. Figure 1 shows a typical measurement. Of the several representations of the correlation function, the most useful is the semi-logarithmic plot ($\log g^{(2)}(t)$ vs. t , middle left). The slope of this almost perfectly straight line is the decay rate of the intensity autocorrelation function; if there were any curvature, it would represent size polydispersity or asphericity.

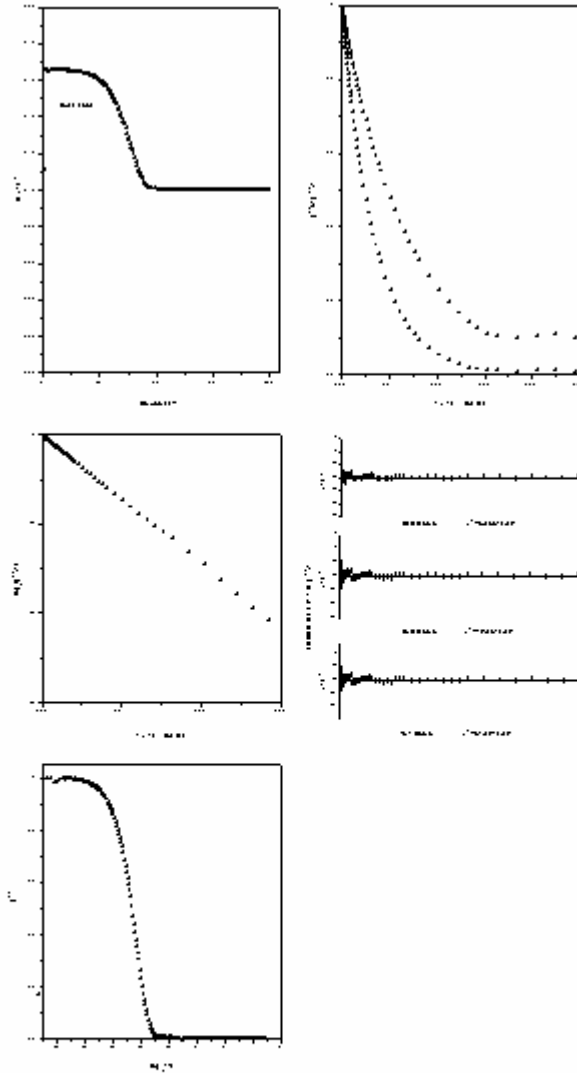


Figure 1. Correlation function in several representations. Top left: raw data in linear/log time format. Top right: normalized 2nd (bottom) and 1st (top) autocorrelation functions in linear/linear format. Middle left: semilogarithmic 2nd order autocorrelation function. Middle right: residuals plots for 1st, 2nd, and 3rd order cumulant fits. The height of the data lines, one for each measured channel, reflects the uncertainty in the measurement. As most such lines touch the horizontal line of zero error, the χ^2 parameter is nearly unity. What deviations occur are small and nearly random.

| | | | |
|--|---------------|----------------|-----------------------|
| CEB 30... | 9021.2091 ... | Sat May 12 13: | P..... |
| Dow larger | | | |
| p = 27 | se = | T = 25.0100°C | u = 0.00463 P |
| $\lambda_s = 6.320\text{\AA}$ | n = 1405 | # Runs: 1 | HEP TIME: 90.57 (SEC) |
| Polymer Analysis Laboratory -- Baton Rouge | | | |

The decay rates were proportional to squared scattering vector, as expected of uniformly sized, spherical particles; see Figure 2. Sometimes, small deviations from uniformity become apparent when $D_{app} = \Gamma/q^2$ is plotted, but not in the case of these particles. Figure 3 shows excellent uniformity, easily the equal of most latex spheres.

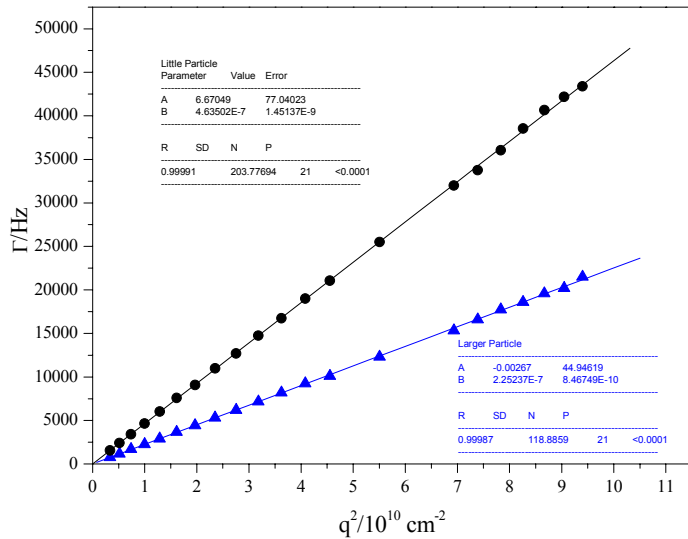
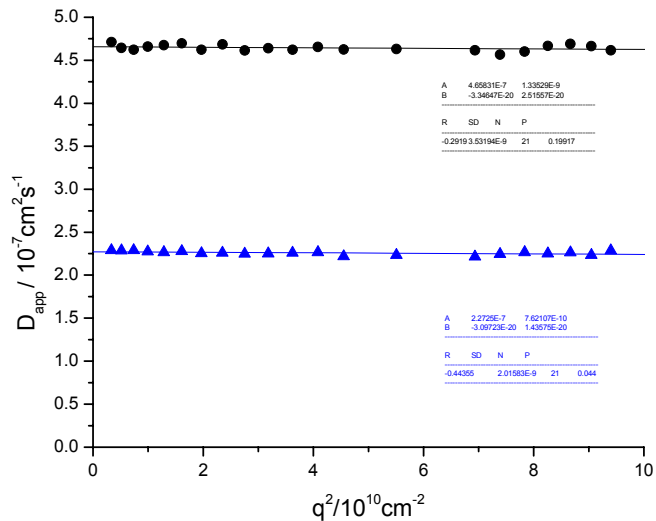


Figure 2. Decay rates plotted against squared scattering vector, showing excellent particle uniformity.

Figure 3. Apparent diffusion coefficients plotted against squared scattering vector, showing excellent particle uniformity.



Although the hydrodynamic radius should be determined in the limit of zero concentration, Figure 4 confirms the absence of any concentration effect in the measured range. The concentrations for this figure were determined by drying the samples. Taken

together, Figures 2-4 suggest that particle sizing would be highly reliable from just one measurement at any experimentally accessible angle and any reasonable concentration.

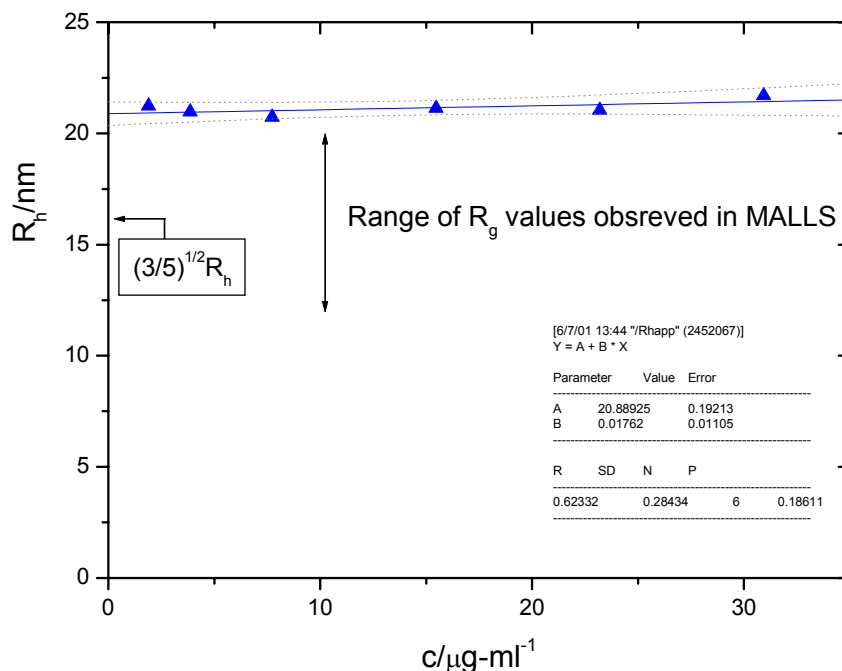


Figure 4. Results do not depend on concentration in the measured range.

GPC/MALLS

Light scattering (at 90 degrees of angle) and differential refractive index (DRI) signals appear in Figure 5. The positive DRI signal corresponding to the particles is very weak, but we compensated by increasing the sensitivity of our detector beyond usual values. The samples supplied contain appreciable quantities of water, evidenced by the negative peaks eluting at long times.

Measurement of molecular weight requires the specific refractive index increment, dn/dc . From the area under the peak associated with either particle, it was noticed that the large and small particles differed in dn/dc . The final dn/dc values used, Table 1, were obtained by calibrating the differential refractometer response with XXX PS-1683 injections of known mass, using 0.185 ml/g as the PS-1683 dn/dc value. Better values--e.g., from our Brice-Phoenix differential refractometer--could be obtained, but only after the water indicated in Figure 5 was removed by vacuum drying, and only if the materials resuspend correctly. Results on drying/resuspension were mixed; while the larger particle resuspended to give a DLS size identical to the original solution, the smaller one did not. Resuspending the smaller particles resulted in a stir opalescent solution. The solution could be filtered through 0.2 μm PTFE filters, and the filtrate (not stir opalescent) contained particles of the same size measured prior to drying.

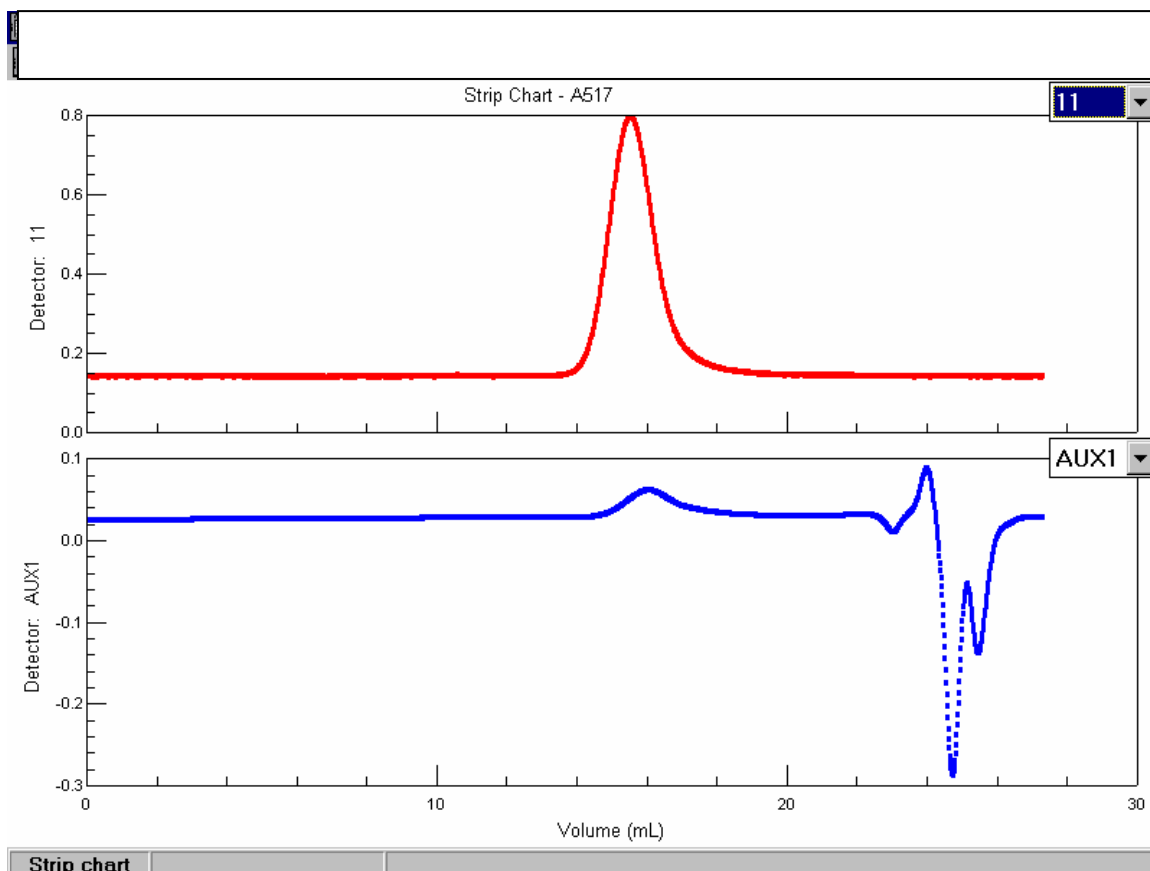


Figure 5. 90° light scattering (top) and DRI (bottom) traces for the smaller particle. One of 3 nearly identical runs.

Apparently, the structures responsible for stir opalescence do not comprise much of the sample, or can be destroyed by filtering. The dried particles were hygroscopic. Brice-Phoenix measurements of dn/dc were deferred until more chemical information about the materials is available, along with larger quantities. Molecular weight and radius values appear in Table 1. The ratio R_h/R_g is slightly higher than expected for solid, spherical particles. This may reflect error in measuring such small R_g values with a long wavelength laser, or it may indicate hydration or nonuniformities in the particles.

Figure 6 reveals details of the molecular architecture for the larger particles. The size depends very little on the molar mass until $M \approx 5 \times 10^6$. After that, the radius increases with mass, following a power law that yields a fractal dimension of 3 within the fairly substantial error. Particle densities can be computed as

$$\rho = \frac{M / N_a}{\frac{4\pi}{3} R^3} \quad (6)$$

where N_a is Avogadro's number. If one assumes $R = (5/3)^{1/2}R_g$, the density ranges from about 0.4 to 0.6 g·ml⁻¹, as shown in Figure 7. Each replicate density curve indicates a rising-then-leveling behavior, consistent with Figure 6. Some caveats are in order. While DAWN instruments, equipped as ours are with 632.8 nm laser sources, can measure sizes in the 10-nm range, errors in baseline, normalization of the multiple detectors and interdetector alignment become critical for these small sizes. The problem is especially challenging for such a narrowly distributed sample; the "bump" observed in two of the three runs probably represents minor interdetector problems associated with the steep rise in the signals.

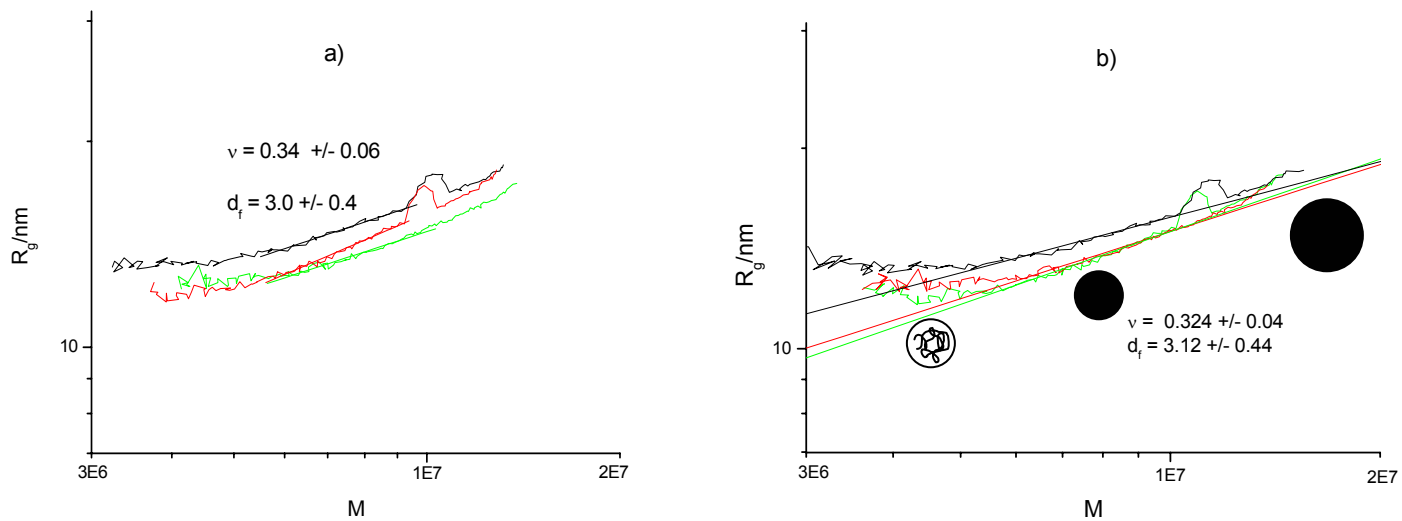


Figure 6. a) Radius of gyration plotted against molecular weight for the larger particle, computed using $dn/dc = 0.164 \text{ ml}\cdot\text{g}^{-1}$. Three replicate runs. b) Same as (a) but dn/dc computed assuming 100% total recovery ($dn/dc = 0.162 - 0.182 \text{ ml}\cdot\text{g}^{-1}$). The increasing particle density, then size, is shown schematically.

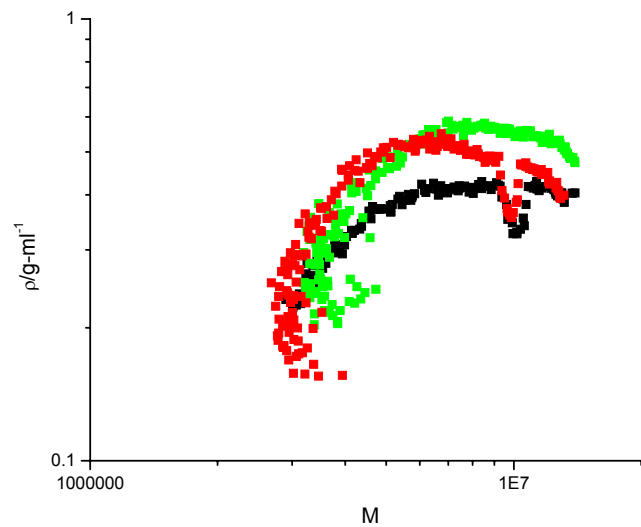


Figure 7. Distribution of particle densities for the larger particle. Same three replicate runs as in Fig. 6.

Figure 8 is analogous to Figure 6, except it is for the smaller particles. Although the run-to-run variation is small, we are reluctant to assign much importance to scaling exponents from such very small particles. The apparent fractal dimensions-- 3.0 ± 0.4 for the larger particles and 2.22 ± 0.38 for the smaller--are almost within error.

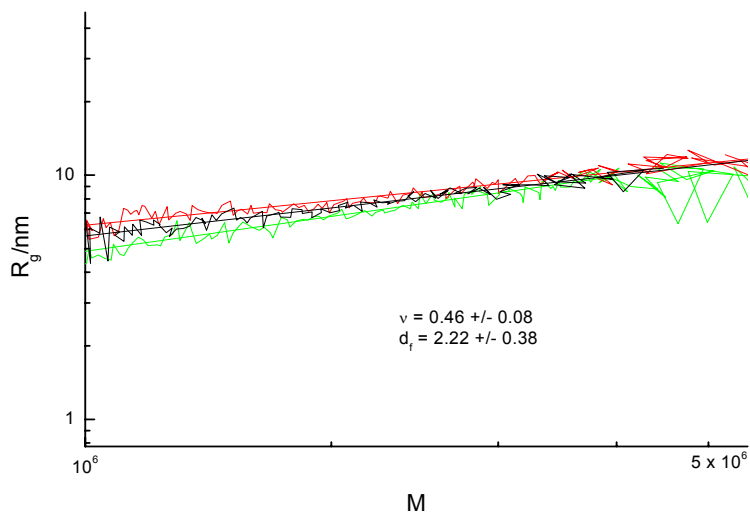


Figure 8. Radius of gyration plotted against molecular weight for the smaller particle, computed using $dn/dc = 0.138 \text{ ml}\cdot\text{g}^{-1}$. Three replicate runs.

Summary

Static and dynamic light scattering measurements reveal the particles to be highly uniform, although some variation of particle density is indicated. Both small and large particles are highly uniform. They would make excellent model particles, and we hope to use what little solution remains to test the agreement between DLS and diffusion ordered NMR spectroscopy (DOSY). The hydrodynamic radii exceed the expectations based on R_g values, by 10% for the larger particles and 10-30% for the smaller particles. The level-then-rising behavior of Figure 6 for the larger particles suggests a distribution in particle density. This should show up in GPC/Viscosity measurements. It would be very interesting to reinvestigate these samples by GPC/MALLS using light of shorter wavelength. The gain on the DAWN amplifiers might need to be reduced, and the DRI sensitivity further increased, to optimize such measurements. Such small particles lie in the linear Guinier regime, so measurements that combine static and dynamic light scattering detection might also be worth pursuing. The stir opalescence observed on resuspending the smaller particles deserves additional attention. Considerable time was spent trying to obtain the specific refractive index increment, dn/dc , by the more reliable Brice-Phoenix instrument, but this was not particularly successful. Additional measurements would be simplified by having the material in solid form. Comparable time was spent trying to measure classical Zimm plots. These were not very successful due to the small size of the particles; shorter wavelengths and possibly higher concentrations would be advisable if these measurements are repeated.

Acknowledgment. This work supported by XXX and the National Science Foundation. This work was done by Dr. Paul Russo, Dr. Rafael Cueto and Ms. Nadia J. Edwin.

Table 1. Summary of Findings

| Parameter | Big | Little |
|--|-----------------------------|-------------------------------|
| R_h/nm (DLS) | 21.2 ± 0.1 | 10.4 ± 0.1 |
| R_g/nm (GPC/MALLS) | 15.3 ± 0.5 | 6.7 ± 1.2 |
| R_h/R_g (DLS and GPC/MALLS) (% difference from $(5/3)^{1/2}=1.291$) | 1.39 ± 0.05 (4-11%) | 1.61 ± 0.28 (2-47%) |
| M_w | $(9.0 \pm 0.1) \times 10^6$ | $(1.40 \pm 0.02) \times 10^6$ |
| M_w/M_n | 1.21 ± 0.01 | 1.28 ± 0.01 |
| ν | 0.34 ± 0.06 | 0.46 ± 0.08 |
| $(dn/dc) / ml\text{-}g^{-1}$ (Astra) | 0.175 ± 0.01 | 0.136 ± 0.006 |
| | | |

Appendix.

Methods

DLS measurements were performed on the "Phoenix" instrument, built in the LSU shops. Samples in 12-mm screw-cap test tubes, which had been cleaned by soap followed by extensive rinsing with water from a Barnstead Nanopure purifier (5 nm spiral wound ultrafilter) and drying, were immersed in a toluene index matching vat to reduce stray light. Typical aperture and pinhole settings were 800 μm and 50 μm respectively. An absorptive beam "stop" was used. The intensity autocorrelation function was obtained with an ALV5000 digital autocorrelator. Decay rates were obtained from third cumulant and single exponential fits (floated baseline). PTFE filters used were (0.2 μm Gelman Acrodisc). Centrifugation for 90 min at 7,000 rpm in a Sorvall HS4 swinging bucket rotor resulted in cleaner samples, but no sedimentation of the particles was observed.

GPC/MALLS experiments were conducted on a Wyatt Dawn DSP, calibrated with toluene as a Rayleigh standard. The Waters 410 differential refractometer was calibrated by the discrete step method using XXX PS1683 as a refractive index standard ($dn/dc = 0.185 \text{ ml/g}$). The column set included a Phenogel 10 MXM (Phenomenex, part number 10H-0201-K0) and Phenogel 10^5 \AA (Phenomenex, part number 10H-0246-K0), both sized at 300 x 7.8 mm. The theoretical plate count with or without the DAWN in place was approximately 7800/foot.

Recommendation for Future Studies

Further investigation of the stir opalescence nature of the solution by electron microscopy will determine whether the solution or particle structure comprises of rods. The solution was stored at room temperature for several months after initial experimentation. Visual investigation revealed most of the stir opalescent property of the solution had disappeared. The sample was prepared and observed under the microscope for indications of any structural patterns, but none was noted. Thus, it was not necessary to perform additional electron microscopy experiments. It was concluded that the structural make-up of the stir opalescence properties was minimal and had disappeared during storage of the sample.

CHAPTER III

Diffusion Ordered Spectroscopy of Water in Hydroxypropyl Cellulose Solutions

Diffusion Ordered Spectroscopy of Water in (Hydroxypropyl) cellulose solutions

Introduction

Hydroxypropyl cellulose, HPC is a water-soluble derivative of native cellulose which is composed of a backbone of anhydroglucose units derived from the original cellulose (β -D-glucose residues in the chair conformation linked together by 1-4 glycosidic bonds).¹ This study have been undertaken to investigate the dynamics of the phase transition of aqueous solutions of HPC (hydroxypropyl cellulose). It is known that aqueous HPC (HPC in water) is a rodlike material that reportedly phase separates during heating and returns to a single phase upon cooling. Diffusion-ordered spectroscopy, DOSY, is used to investigate the possible existence of “bound” water in the HPC system. The phase separation temperature was established by performing temperature experiments (25°C – 60°C) of 0.1 and 1 percent aqueous HPC solutions.

Background

Self-diffusion is a measure of the translational motion of a molecule. Diffusion is seen to relate to molecular size by the Stokes-Einstein equation given below:

$$D = \frac{kT}{f} \quad (1)$$

where k is the Boltzmann's constant, T is the temperature and f is the friction coefficient, for a solvent of viscosity η , the friction factor is given by $f = 6\pi\eta R_h$. For a true sphere, the hydrodynamic radius, R_h , equals the actual radius, R . The hydrodynamic radius is determined from the diffusion coefficient, D , according to equation 1 above.

$$R_h = kT/6\pi\eta D \quad (2)$$

The diffusion coefficient can be used to determine the size and shape of individual molecules as well as molecular aggregates. Diffusion-ordered spectroscopy is used to measure self-diffusion coefficient of molecules by separating NMR signals of different species. In this experiment, spin echo spectra measured with different pulsed (magnetic) field gradient strengths and signal decays are analyzed to provide various diffusion coefficients. Nuclear spins that are within a homogenous magnetic field precess at the Larmor frequency according to the equation:

$$\omega_o = \gamma B_o \quad (3)$$

where ω_o is the Larmor frequency, γ is the gyromagnetic ratio and B_o is the strength of the magnetic field.

Results and Discussion

DOSY. Figure 1 shows the 0.1% HPC solution in water has a phase transition occurring at $\sim 41^\circ\text{C}$. This is evident by the slight “V” seen in the navy blue diamond data points in the plot. The pink data points indicate results obtained by an earlier experiment done by Mazidah Mustafa. The trends observed in both data sets are similar.

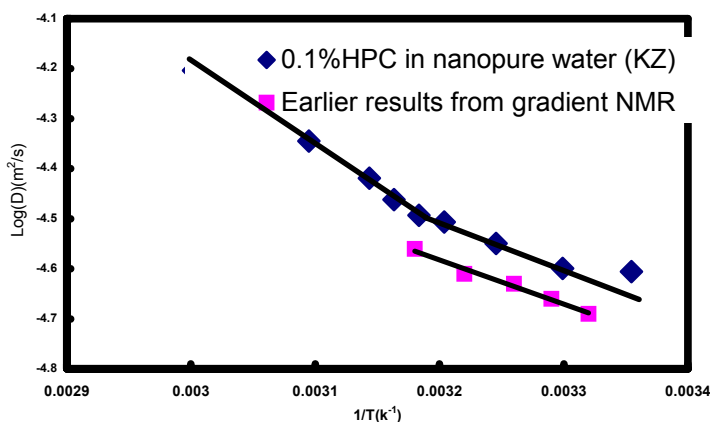


Figure 1. Phase Transition of 0.1% HPC in water.

Figure 2 shows the 1% HPC has two distinct slopes, which is not indicative of a phase transition point. A possible reason for the discrepancy could be attributed to the HPC precipitating out of solution and forming a gel, which could interfere with the NMR results. To verify that claim, the phase transition of water was determined to find out if water was affecting the HPC. The results obtained for water, shown in Figure 3, was a straight line as expected. Thus, the results obtained for the 1% HPC which is similar to water is still questionable.

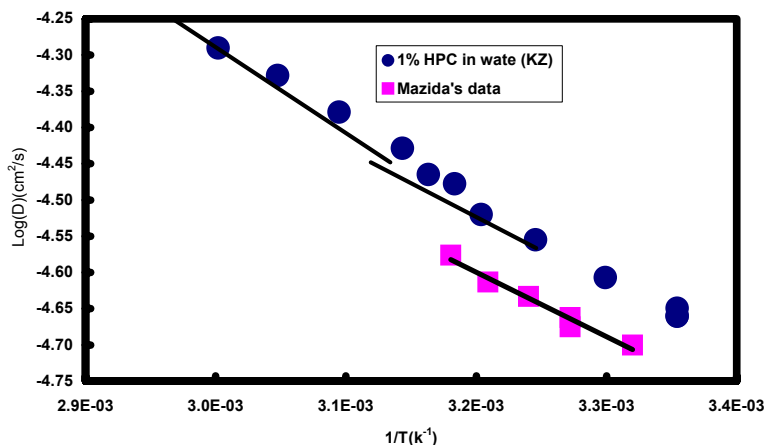


Figure 2. Phase Transition of 1% HPC in water.

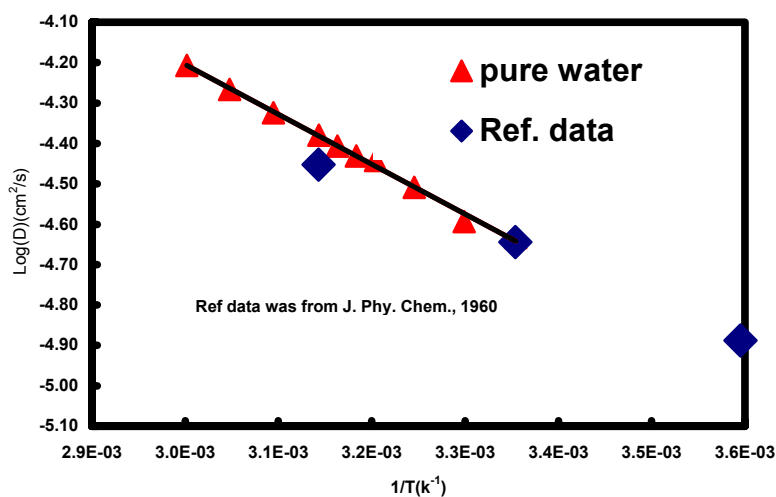


Figure 3. Phase Transition of water.

Appendix

Materials and Methods

The Hydroxypropyl cellulose used in this study was HPC powder with a molecular weight $M_w \approx 300,000$ purchased from Scientific Polymer Products Inc., CAS# 9004-64-2. Aqueous HPC solutions of 0.1 and 1 percent concentrations were prepared by dissolving it in deionized water from a Barnstead Nanopure purifier (5 nm spiral wound ultrafilter) for about one week duration. The solutions were then pipeted into 5mm regular walled NMR tubes. Diffusion-ordered spectroscopy measurements of the self-diffusion coefficient were carried out on a Bruker DPX400 NMR Spectroscopy operating at 400 MHz for protons. The temperature was set over a range of 25°C – 60°C.

Recommendations for Future Studies

A perplexing problem that still remains after performing this experiment is the fact that the 1% HPC plot shown in Figure 2 above has two distinct slopes, which is not indicative of a phase transition point. This problem can be further explored by repeating the experiment with HPC solution concentrations of 0.5 and 2% respectively. The additional data points may help provide a clearer picture of the trend in the results. One problem encountered while performing the experiment is the precipitation of the HPC while the experiment was still running. This can be corrected by placing glass-fiber in the bottom of the NMR tube prior to placing the sample in the tube. Similar studies can also be undertaken with a different solvent, for example D₂O for comparison.

Acknowledgment. This work was done by R. Cong, Rae-lynn Poirrier, Frank Zhou.

References:

Longworth, L. G., *Journal of Physical Chemistry*, **1960**, vol.64, p. 1914-1917.

Mustafa, Mazidah. B. *Molecular Dynamics of Solutions Containing Water-soluble Semiflexible Polymer*. Doctoral dissertation. Louisiana State University, Baton Rouge, LA, 1990.

Samuels, R. J., *Journal of Polymer Science*, **1969**, A2, vol.7, 1197.